

Radiative Prandtl–Eyring Fluid Flow With Magnetohydrodynamics Over A Stretching Sheet Under Convective Heating: A Keller Box Method Investigation

K. Keziya^{1*}, and Ch. Suresh kumar²

^{1*}Department of Mathematics, DS Govt. Degree College, Ongole, Andhra Pradesh-523001, India.

²Department of Mathematics, Ch. Suresh Kumar, KRK Govt. Degree college, Addanki, Andhra Pradesh – 523201, India.

*Corresponding Author: K. Keziya

*Department of Mathematics, DS Govt. Degree College, Ongole, Andhra Pradesh-523001, India.

Abstract:

This work sheds light on the intricate interdependencies within the magneto-hydrodynamic boundary layer flow of a Prandtl-Eyring fluid with heat effects. The numerical solutions and resulting trends provide valuable insights for applications in fields such as materials science, engineering, and physics. The partial differential Equations describing the momentum and heat equations are converted into ordinary differential equations which are nonlinear, with the assistance of similarity transformations. Numerical solution for the above equations is brought forth by employing the Keller-Box method. The out puts of our study is explained through tables and graphs. It is seen that there is uplift in velocity profiles and a drop in temperature profiles with an increase in Fluid parameter λ . Furthermore, the thickness of thermal boundary layer increases because of the increase in Biot number Bi as well as thermal Radiation R .

Keywords: MHD, radiation, Prandtl – Eyring fluid, convective heating, Keller box method.

Introduction

Numerous industrial processes, ranging from extrusion and paper production to fiberglass manufacturing, leverage the principles of boundary layer flows on the surfaces of elongated objects, often intertwined with heat transfer analyses. Further also in some industries for the processes such as hot rolling, condensation process, crystal growing, polymer sheets, artificial fibers and plastic films etc. Due to its vast applications the researchers are curious to study the boundary layer problems. Sakiadis [28] was the very first researcher who studied about boundary layer flow over a stretched surface moving with constant velocity. Later his work was extended by Ericsson et al. [6] also by Chen and Char [4]. Elbashbeshy [5] studied the effect of heat of a linearly stretching sheet subject to blowing or suction. Some fluids used in industries are molten polymers, biological fluids, lubricants, mud and some fluids occurring naturally such as animal blood all are non-Newtonian in nature i.e., which do not have a direct relationship between stress and deformation rate. There are some non-Newtonian fluid models namely, Powell –Eyring, power law, Maxwell, Reynaldo's, Vogel's model, and micropolar fluid models. power law model takes empirical relation from kinetic theory of liquid Powell–Eyring fluid over a stretching surface and it condenses to Newtonian at high and low shear rates. Akbar et al. [2] revealed in his study on Powell–Eyring fluid over a stretching surface in the presence of magnetic field that the velocity profile is directly proportional to magnetic flux and Powell–Eyring fluid parameters. Malik et al. [18] analyzed the models, namely Reynaldo's, Vogel's and Powell– Eyring models on a stretching cylinder and observed that boundary layer reduced for

large Prandtl number values. Also, they analyzed that velocity profile increased by enhancing the values of suction parameter. The temperature profile reduces for large values of suction parameter. Ara et al. [3] illustrated the flow of Powell–Eyring fluid over a shrinking surface told velocity profile increased with the mass suction increment, while temperature profile showed opposite behavior. Also, the boundary layer thickness reduced with increase in Prandtl number. Nadeem and Saleem [21] observed the free and forced convection flow past a stretching cone in the existence of mass and heat transfer. They observed that tangential velocity has opposite behavior for flow parameters. Moreover, they observed that skin friction coefficient increased due to the increment in ratio of buoyancy forces to flow parameter. Hayat et al. [12] examined the comparison of series and numerical solutions for flow of Powell–Eyring fluid with Newtonian heating. Also, they considered the internal heat generation and absorption. Malik et al. [96] used Keller box method and analyzed the MHD flow of tangent hyperbolic fluid over a stretching cylinder. In references [22, 27], authors investigated the Powell–Eyring fluid model in different physical conditions. The magneto-hydrodynamics (MHD) of an electrically conducting fluid is encountered in many problems in geophysics, astrophysics, engineering applications and other industrial areas. Focusing on moving and stretching surfaces, Rajesh Kumar et al. [23] studied MHD flow and heat transfer on a continuously moving vertical plate and Ishak et al. [15] analyzed the same case over a stretching sheet. Khan et al. [16] studied the impact of heat transfer on the Newtonian MHD boundary layer of Powell–Eyring fluid over a stretching sheet. They made it clear, for higher values of fluid parameter and Hartmann number, velocity profile decreases. Hussain et al. [14] confabulated that magneto hydro dynamic Sisko fluid over a stretching cylinder by employing shooting method asserted the effects of viscous dissipation on energy equation. At recent days, Gangadhar et al. [10] made a study on the impacts of chemical reaction over tangent hyperbolic fluid on a stretched surface and concluded that in the region of boundary layer the chemical reaction impacts the concentration distribution. Again, Gangadhar et al. [9] examined, by using spectral relaxation technique the impacts of viscous dissipation as well as heat absorption or generation on unsteady boundary layer flow of a nanofluid over a stretched surface and gave conclusion that the heat source/sink lowers heat transfer rate all over the boundary layer.

The devices which are operated at high temperature like gas turbines, nuclear power plants, satellites, space vehicles, the radiation effect on magneto hydrodynamics flow absolutely important. Takhar et al. [31] scrutinized the effect of radiation on magneto hydrodynamics free-convection flow of a gas over a semi-infinite vertical plate. Hossain and Takhar [13] examined the radiation effect on a mixed convection flow of an optically depth uniformity flow over a vertically heated porous plate with uniform surface temperature and uniform suction rate where radiation is included by supposing Rosseland diffusion approximation. Ghaly [11] evaluate the effect of radiation over a stream line flow, and Raptis and Massalas [25] and El-Aziz [1] explored the above which were not steady as well. Shateyi et al. [30] analyzed a MHD flow by radiation heat transfer on a vertical plate. Researchers Raptis and Kafoussias [24], Sattar et al. [29], Kim [17], and Whitaker [32] gave results regarding the radiation of heat transfer in porous medium. In manufacturing of polymers the effect of radiation plays a crucial role. Mukhopadhyay [20] examined the mixed convection flow and transfer of heat upon a porous stretching surface in a porous medium. The eventuality and effects of MHD as well as radiation on a boundary layer flow and heat transfer study along vertical elongated sheet is observed by Ferdows et al. [7]. Their observation ratifies and approves the fact that Nusselt number falls down with the influence of radiation. Ganesh kumar et al. [8] tested non linear thermal radiation and MHD out come on double diffusive mixed convection boundary layer flow of visco elastic Nanofluid over a stretched sheet. Raptis [26] investigated the radiation as well as MHD effects on boundary layer flow over a vertical plate.

Hence forth, this detailed work outlines a theoretical study and scrutinization of MHD flow belongs to Prandtl –Eyring fluid over a stretching sheet. A mathematical model was made by considering the heat effects both radiation and convection. For numerical solution we used Keller-Box method. The

velocity and temperature profiles are compared for both Prandtl-Eyring and Newtonian fluids and variations of these profiles for different parameters are also examined.

Mathematical Analysis

We consider a Prandtl-Eyring fluid flow which is two dimensional, non –Newtonian, steady, incompressible upon an elongated or a stretching sheet. This stretching is linear along x axis and the fluid distributed throughout the positive half plane of vertical axis. We applied Magnetic field normally to this flow. The physical diagram and coordinate system of the problem is illustrated in figure 1.

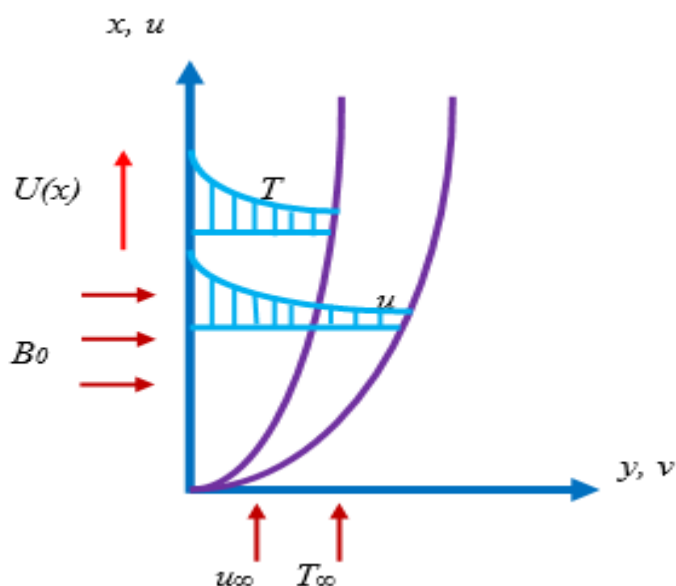


Figure 1: Geometry of the problem.

Here mass, momentum is conserved. So their equations are given by

$$\nabla \cdot \mathbf{V} = 0, \quad (1)$$

$$\rho \frac{d\mathbf{V}}{dt} = \text{div}\mathbf{H} + \mathbf{J} \times \mathbf{B}, \quad (2)$$

$$\rho C_p \frac{dT}{dt} = K(\nabla^2 T) \quad (3)$$

Here $\mathbf{V}, \mathbf{H}, \mathbf{J}, \rho$ are the velocity field, Cauchy stress tensor, electric current density and fluid density respectively.

$$\mathbf{H} = -p\mathbf{I} + \mu\mathbf{S} \quad (4)$$

Here $p, \mathbf{I}, \mu, \mathbf{S}$ are fluid pressure, identity tensor, dynamic viscosity and extra stress tensor of the fluid respectively.

$$S = \frac{A \sinh^{-1} \left(\frac{1}{C} \sqrt{\frac{1}{2} \text{tr}(\mathbf{A}_1^2)} \right)}{\sqrt{\frac{1}{2} \text{tr}(\mathbf{A}_1^2)}} \quad (5)$$

Here both A and C are the fluid parameters. From equations (4), (5) and with approximations of boundary layer, equations (1), (2) and (3) becomes

$$\frac{\partial u}{\partial x} + \frac{\partial v}{\partial y} = 0, \quad (6)$$

$$u \frac{\partial u}{\partial x} + v \frac{\partial u}{\partial y} = \frac{A}{\rho C} \frac{\partial^2 u}{\partial y^2} - \frac{A}{2\rho C^3} \left(\frac{\partial u}{\partial y} \right)^2 \frac{\partial^2 u}{\partial y^2} - \frac{\sigma B^2}{\rho} u. \quad (7)$$

$$u \frac{\partial T}{\partial x} + v \frac{\partial T}{\partial y} = \frac{\nu}{\rho c_p} \frac{\partial^2 T}{\partial y^2} - \frac{1}{\rho c_p} \frac{\partial q_r}{\partial y}. \quad (8)$$

Here velocity components are u , v and σ is electrical conductivity.

$$\left. \begin{aligned} u = U(x) = ax, \quad v = 0 \quad \text{at } y = 0 \\ u \rightarrow 0 \quad \text{at } y \rightarrow \infty \end{aligned} \right\} \quad (9)$$

Above, $U(x)$ is fluid's stretching velocity.

Choose $\psi(x)$ the stream function such as $u = \frac{\partial \psi}{\partial y}$, $v = -\frac{\partial \psi}{\partial x}$ and transformations

$$\left. \begin{aligned} \eta = \sqrt{\frac{a}{\nu}} y \\ \psi = \sqrt{a\nu} x f(\eta) \end{aligned} \right\} \quad (10)$$

Here η , f are independent and dependent variables, ν is kinematic viscosity.

Now the eq. (7) and (8) changes to

$$\lambda f''' - \lambda \xi f''^2 f''' - f'^2 + ff'' - Mf' = 0 \quad (11)$$

$$\alpha \theta'' + \text{Pr} f \theta' = 0 \quad (12)$$

$$f(0) = 0, \quad f'(0) = 1, \quad \theta'(0) = -Bi(1 - \theta(0)), \quad f'(\infty) = 0, \quad \theta(\infty) = 0 \quad (13)$$

Where

$$\lambda = \frac{A}{\mu C}, \quad \xi = \frac{a^3 x^2}{2C^2 \nu}, \quad M = \frac{\sigma B^2}{a\rho}, \quad \alpha = \left(1 + \frac{4}{3} Rd \right) \quad (14)$$

We have the skin friction coefficient

$$C_f = \frac{\tau_w}{\frac{1}{2} \rho U^2}. \quad (15)$$

Here τ_w , the shear stress at the wall is given by

$$\tau_w = \frac{A}{C} \left(\frac{\partial u}{\partial r} \right)_{y=0} - \frac{A}{6C^3} \left(\frac{\partial u}{\partial r} \right)_{y=0}^3 \quad (16)$$

By using dimensionless variables the skin friction transforms to

$$\frac{1}{2} C_f \text{Re}_x^{\frac{1}{2}} = \lambda f''(0) - \frac{\lambda \xi}{3} [f''(0)]^3 \quad (17)$$

Where $\text{Re}_x = \frac{xU(x)}{\nu}$ is the Reinhold's number.

Numerical procedure to get the solution

Kellor –Box method is applied to compute the Eqs. (11) and (12). In this method we introduced the new dependent variables p, q, r and t in order to convert the second order D.E into first order D.E such as,

$$f' = p \quad (18)$$

$$p' = q \quad (19)$$

$$q' = r \quad (20)$$

$$\theta' = t \quad (21)$$

After using these variables eq.(11)and (12) modifies to

$$\lambda q' - \lambda \xi q^2 q' + fq - Mp - p^2 = 0 \quad (22)$$

$$\alpha t' + \text{Pr} ft = 0 \quad (23)$$

Using central difference derivatives at mid point,

$$\frac{f_j - f_{j-1}}{h_j} = \frac{p_j + p_{j-1}}{2} \quad (24)$$

$$\frac{p_j - p_{j-1}}{h_j} = \frac{q_j + q_{j-1}}{2} \quad (25)$$

$$\frac{\theta_j - \theta_{j-1}}{h_j} = \frac{t_j + t_{j-1}}{2} \quad (26)$$

Now the eqs.(22) and(23) re modifies to

$$\lambda(q_j - q_{j-1}) - \frac{h_j}{2} \lambda \xi (rq^2)_{j-\frac{1}{2}} + \frac{h_j}{2} f_{j-\frac{1}{2}} q_{j-\frac{1}{2}} - \frac{h_j}{2} \left(P_{j-\frac{1}{2}} \right)^2 - \frac{h_j}{2} MP_{j-\frac{1}{2}} = U_{j-\frac{1}{2}} \quad (27)$$

$$\alpha(p_j - p_{j-1}) + \text{Pr} \left\{ h_j \left[f_{j-\frac{1}{2}} \left(\frac{p_j + p_{j-1}}{2} \right) \right] + h_j p_{j-1} \left(\frac{f_j + f_{j-1}}{2} \right) \right\} = 0 \quad (28)$$

Here

$$U_{j-\frac{1}{2}} = -\lambda(q_j - q_{j-1}) + \frac{h_j}{2} \lambda \xi (rq^2)_{j-\frac{1}{2}} - \frac{h_j}{2} f_{j-\frac{1}{2}} q_{j-\frac{1}{2}} + \frac{h_j}{2} \left(P_{j-\frac{1}{2}} \right)^2 + \frac{h_j}{2} MP_{j-\frac{1}{2}} \quad (29)$$

Here

$$\alpha = 1 + \frac{4}{3} Rd$$

The new conditions of the boundary are

$$f_0 = 0, p_0 = 1, \theta_0 = 1, p_J = 0, \theta_J = 0. \quad (30)$$

Solving the higher order non-linear equations (24) to (28), by using Newton's method

$$f_j^{(k+1)} = f_j^{(k)} + \delta f_j^{(k)}, p_j^{(k+1)} = p_j^{(k)} + \delta p_j^{(k)}, q_j^{(k+1)} = q_j^{(k)} + \delta q_j^{(k)}, \theta_j^{(k+1)} = \theta_j^{(k)} + \delta \theta_j^{(k)},$$

$$t_j^{(k+1)} = t_j^{(k)} + \delta t_j^{(k)}. \quad (31)$$

Where k=0, 1, 2.....

Now the above system of equations re arranged to

$$\delta f_1 - \delta f_0 - \frac{h_1}{2} \delta p_1 - \frac{h_2}{2} \delta p_0 = (s_1)_{j-\frac{1}{2}} \quad (32)$$

$$\delta p_1 - \delta p_0 - \frac{h_1}{2} \delta q_1 - \frac{h_2}{2} \delta q_0 = (s_2)_{j-\frac{1}{2}} \quad (33)$$

$$\delta \theta_1 - \delta \theta_0 - \frac{h_1}{2} \delta t_1 - \frac{h_2}{2} \delta t_0 = (s_3)_{j-\frac{1}{2}} \quad (34)$$

$$c_1 \delta q_j + c_2 \delta q_{j-1} + c_3 \delta f_j + c_4 \delta f_{j-1} + c_5 \delta p_j + c_6 \delta p_{j-1} = (s_4)_{j-\frac{1}{2}} \quad (35)$$

$$d_1 \delta t_j + d_2 \delta t_{j-1} + d_3 \delta f_j + d_4 \delta f_{j-1} = (s_5)_{j-\frac{1}{2}} \quad (36)$$

Here,

$$(c_1) = \lambda - \frac{\lambda \xi}{2} q_{j-\frac{1}{2}}^2 - \frac{h_j}{2} \lambda \xi (qr)_{j-\frac{1}{2}} + \frac{h_j}{4} f_{j-\frac{1}{2}}$$

$$(c_2) = -\lambda + \frac{\lambda \xi}{2} q_{j-\frac{1}{2}}^2 - \frac{h_j}{2} \lambda \xi (qr)_{j-\frac{1}{2}} + \frac{h_j}{4} f_{j-\frac{1}{2}}$$

$$c_3 = \frac{hq_{j-\frac{1}{2}}}{4}$$

$$c_4 = c_3$$

$$c_5 = -\frac{h}{2} P_{j-\frac{1}{2}} - \frac{hM}{4}$$

$$c_6 = c_5$$

(37)

$$d_1 = \alpha + \frac{h_j Pr}{2} f_{j-\frac{1}{2}}$$

$$d_2 = -\alpha + \frac{h_j \text{Pr}}{2} f_{j-\frac{1}{2}} \quad d_3 = \frac{h_j \text{Pr}}{2} f_{j-\frac{1}{2}} \quad (38)$$

$$d_4 = d_3$$

$$(s_1)_{j-\frac{1}{2}} = (f_{j-1} - f_j) + \left(\frac{p_j + p_{j-1}}{2} \right) h_j \quad (39)$$

$$(s_2)_{j-\frac{1}{2}} = (p_{j-1} - p_j) + \left(\frac{q_j + q_{j-1}}{2} \right) h_j \quad (40)$$

$$(s_3)_{j-\frac{1}{2}} = (\theta_{j-1} - \theta_j) + \left(\frac{t_j + t_{j-1}}{2} \right) h_j \quad (41)$$

$$(s_4)_{j-\frac{1}{2}} = -\lambda h_j r_{j-\frac{1}{2}} + \frac{h_j}{2} \left(\lambda \xi r_{j-\frac{1}{2}} \left(q_{j-\frac{1}{2}} \right) \right)^2 - f_{j-\frac{1}{2}} q_{j-\frac{1}{2}} + \left(P_{j-\frac{1}{2}} \right)^2 + MP_{j-\frac{1}{2}} + U_{j-\frac{1}{2}} \quad (42)$$

$$(s_5)_{j-\frac{1}{2}} = +\alpha(t_{j-1} - t_j) - \frac{h_j}{2} f_{j-\frac{1}{2}}(t_j + t_{j-1}) - \frac{h_j}{2} t_{j-\frac{1}{2}}(f_j + f_{j-1}) \quad (43)$$

With boundary conditions

$$f_0 = 0, \quad \delta p_0 = 0, \quad \delta p_j = 0. \quad \delta t_j = 0 \quad (44)$$

The system of linear differential equations (32) to (36), is converted into block tri-diagonal matrix structure. Normally this structure contains constants or variables, but here it contains block matrices. On changing the equations (32) to (36) in matrix vector form,

$$A\delta = s$$

$$[A] [\delta] = [s] \quad (45)$$

Here the entries of A, δ, s are given by

$$[A_1] = \begin{bmatrix} 0 & 0 & 1 & 0 & 0 \\ \frac{-h_1}{2} & 0 & 0 & \frac{-h_1}{2} & 0 \\ 0 & \frac{-h_1}{2} & 0 & 0 & \frac{-h_1}{2} \\ c_2 & 0 & c_3 & c_1 & 0 \\ 0 & d_2 & d_3 & 0 & d_1 \end{bmatrix}$$

For $j= 2, 3, 4, \dots, J$

$$[A_j] = \begin{bmatrix} \frac{-h_j}{2} & 0 & 1 & 0 & 0 \\ -1 & 0 & 0 & \frac{-h_j}{2} & 0 \\ 0 & -1 & 0 & 0 & \frac{-h_j}{2} \\ (c_6)_j & 0 & (c_3)_j & (c_1)_j & 0 \\ 0 & 0 & (d_3)_j & 0 & (d_1)_j \end{bmatrix}$$

$$[B_j] = \begin{bmatrix} 0 & 0 & -1 & 0 & 0 \\ 0 & 0 & 0 & \frac{-h_j}{2} & 0 \\ 0 & 0 & 0 & 0 & \frac{-h_j}{2} \\ 0 & 0 & (c_4)_j & (c_2)_j & 0 \\ 0 & 0 & (d_4)_j & 0 & (d_2)_j \end{bmatrix}$$

$$[C_1] = \begin{bmatrix} \frac{-h_1}{2} & 0 & 0 & 0 & 0 \\ 1 & 0 & 0 & 0 & 0 \\ 0 & 1 & 0 & 0 & 0 \\ c_5 & 0 & 0 & 0 & 0 \\ 0 & 0 & 0 & 0 & 0 \end{bmatrix}$$

And the entries of

$$[\delta_1] = \begin{pmatrix} \delta q_0 \\ \delta t_0 \\ \delta f_1 \\ \delta q_1 \\ \delta t_1 \end{pmatrix}$$

For $j = 2, 3, 4, \dots, J$

$$[\delta_j] = \begin{pmatrix} \delta p_1 \\ \delta \theta_1 \\ \delta f_2 \\ \delta q_2 \\ \delta t_2 \end{pmatrix} \quad [s_j] = \begin{pmatrix} s_1 \\ s_2 \\ s_3 \\ s_4 \\ s_5 \end{pmatrix} \quad J = 1, 2, 3 \dots J.$$

The convergence criterion for obtaining the solution for this Block-tridiagonal matrix is $|\delta v_0^i| \leq \varepsilon_1$

Here ε_1 is small given value. This procedure is repeated until it satisfies this criteria and the procedure involved in this solution is the Thomas algorithm.

Results and conclusions

Here we study the boundary layer flow of Prandtl-Eyring fluid upon elongated sheet. Both the boundary layers momentums as well as thermal boundary layers are checked in the presence of

transverse magnetic field. The thermal radiation effect and convective heating on boundary is examined by using Keller-Box method". Also our reports are compared with existing ones of Akbar et al. [2], Malik et al. [18] and Hussain et al. [14] via table 1 and all values are agree with those values. For numerical results and conclusion we considered $M = 0$, $\lambda = 4$, $\xi = 0.5$, $Rd = 0.4$, $Pr = 0.72$, $Bi = 0.2$. Figure 2 and 3 convey the temperature and velocity profiles of Newtonian and Prandtl-Eyring model. The figure indicates a significantly higher magnitude of velocity for the Prandtl-Eyring fluid model compared to the Newtonian model. This disparity can be attributed to the fact that the Prandtl-Eyring fluid exhibits shear thinning behavior, wherein the viscosity decreases with the shear rate. This characteristic leads to an increase in fluid velocity and a corresponding decrease in fluid temperature.

Figure (4) interprets magnetic field parameter's (M) behavior upon velocity profiles. It is a clear that the transverse magnetic field cuts down the fluid velocity internally inside the momentum boundary layer. Magnetic field produces electricity in the flow as a result Lorentz force is exerted on the flow and the resistive nature of this force opposes the fluid motion and consequently the velocity $f'(\eta)$ decreases.

Figure (5) depicts that if magnetic field parameter values increase the temperature profiles also increases. Since the momentum thickness of boundary layer is a function of decreasing magnetic field parameter and due to presence of Lorentz force heat is produced which raises the thickness of the thermal boundary layer substantially leading to raise the temperature profile.

Figure-6 shows the effect of the fluid parameter λ on velocity profile. The velocity profile shows a supplement rise with increasing λ , a raise in λ causes a fall in viscosity that gives rise to the uplift of the velocity field.

Figure-7 explains the action of λ upon the temperature as the increase in λ , the temperature profile along with thermal boundary layer thickness reduces since greater values of λ results in curtailment of the fluid viscosity. Hence, temperature falls down takes place.

Figure (8) Shows, raise in radiation parameter increases the temperature profile. The radiation parameter Rd is liable for increasing thermal boundary layer thickness. So it empowers and allows the fluid from the flow region to dispense heat energy, as a result of this heating of the system takes place. The fact is authentic and correct because Rosseland approximation delivers a rise in temperature.

Figure (9) demonstrates the aspect of the Biot number Bi on the temperature field. It is remarked that there is a rise in temperature for large Biot numbers Bi . On account of fact, as we increase the Bio number, the heat transfer coefficient also increases which is bound to elevate and give rise to temperature profile. Which supports the statement, an Increase in Biot number also accounts to a thermal slip at the wall.

Figure (10) presents the temperature profiles for various values of Prandtl number. The Prandtl number Pr , explains the momentum and thermal diffusivity fraction. It is discovered and seen that when we Increase the Prandtl number Pr , thickness of thermal boundary layer decreases means temperature decreases. The analysis behind this is that lower the values of Prandtl number Pr , corresponding thermal conductivities increases so heat radiates away from the heated plate briskly. The changes in skin friction coefficient for different values of magnetic parameter M and fluid Parameter is demonstrated in Fig 11. It's seen that the coefficient of skin friction decreases when we increase λ , and increases when M is increased. Therefore, greater values of M can be brought into account for the inclination of coefficient of skin friction. Diagrams 12 and 13 depicts that the values of local Nusselt number increases for increasing values of λ and Bi , whereas decreases by increasing M and Rd . So, by choosing suitable values of λ and Bi we can cool the machines in different industries.

Conclusions

In the study of MHD Prandtl- Eyring fluid model over stretching sheet by considering the effects both radiation and convection, we are given the following observations.

1. Newtonian fluids typically demonstrate a more gradual flow compared to Prandtl-Eyring fluids in terms of velocity.
2. Increasing the fluid parameter generally boosts velocity, while a rise in the magnetic parameter tends to reduce velocity.
3. Higher Biot numbers are associated with an increase in wall temperature and simultaneous induction of thermal slip.
4. The skin friction coefficient decreases with an increase in λ and increases with a rise in M .
5. Raising the value of Rd leads to a reduction in the local Nusselt number.

The current study solves the problems related to the fluid flows over stretching surfaces mainly in polymeric sheets, thinning of copper wires, annealing and food processes.

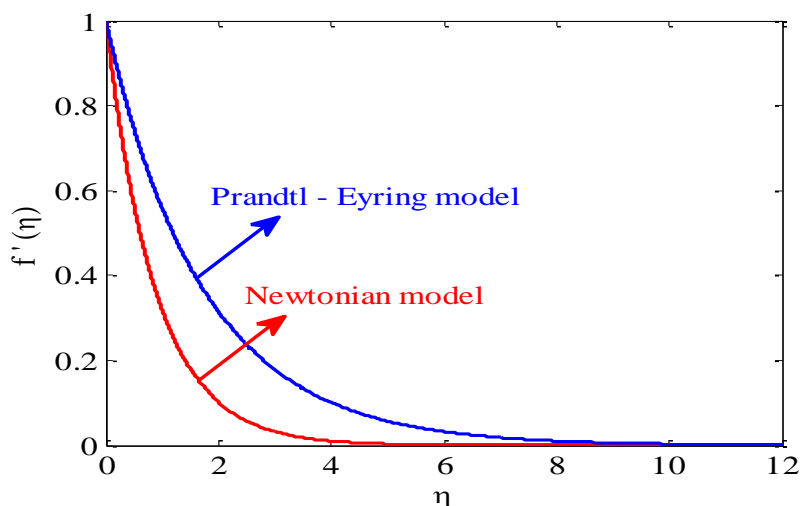


Figure 2: Newtonian model verses Prandtl – Eyring model on velocity profiles $f'(\eta)$.

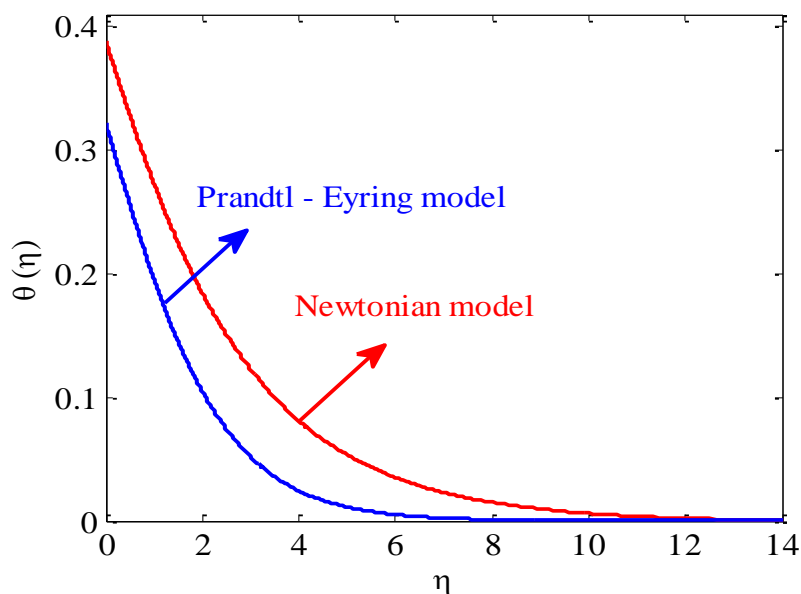


Figure 3: Newtonian model verses Prandtl – Eyring model on temperature profiles $\theta(\eta)$.

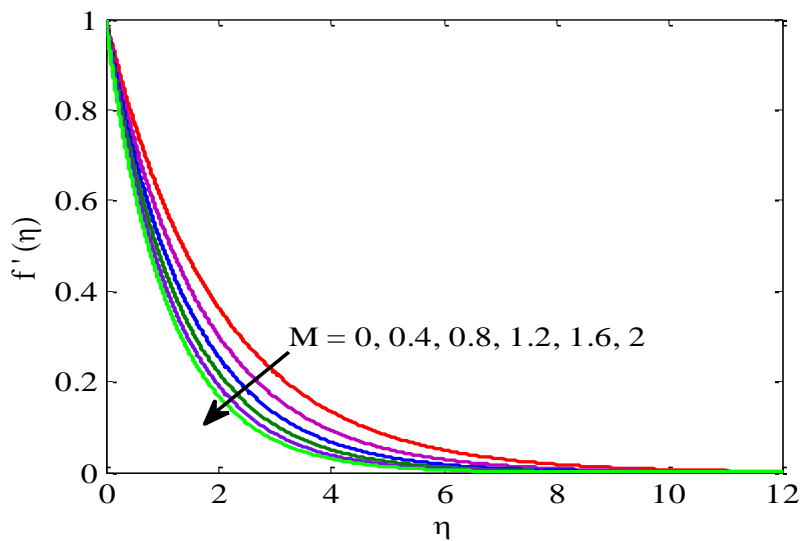


Figure 4: Velocity profiles $f'(\eta)$ under different values of M .

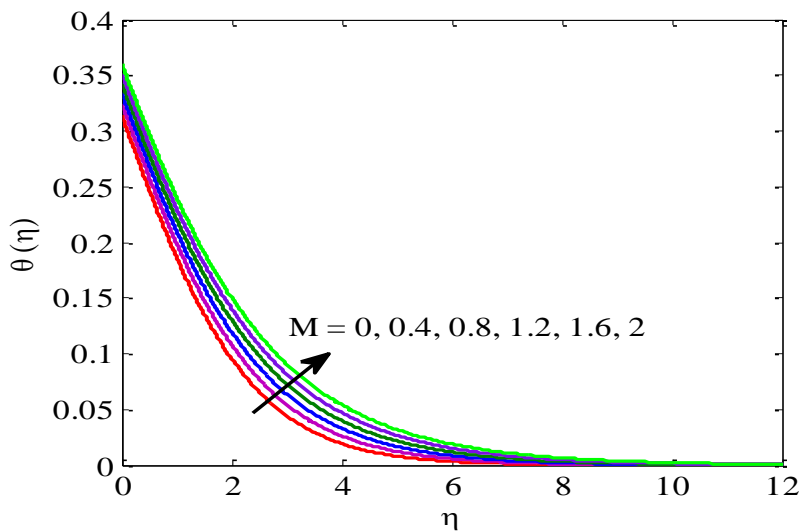


Figure 5: Temperature profiles $\theta(\eta)$ under different values of M .

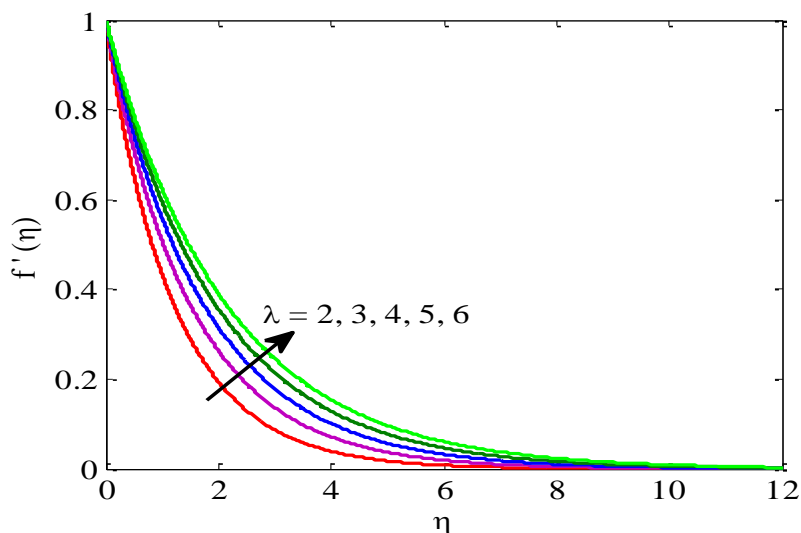


Figure 6: Velocity profile $f'(\eta)$ under different values of λ .

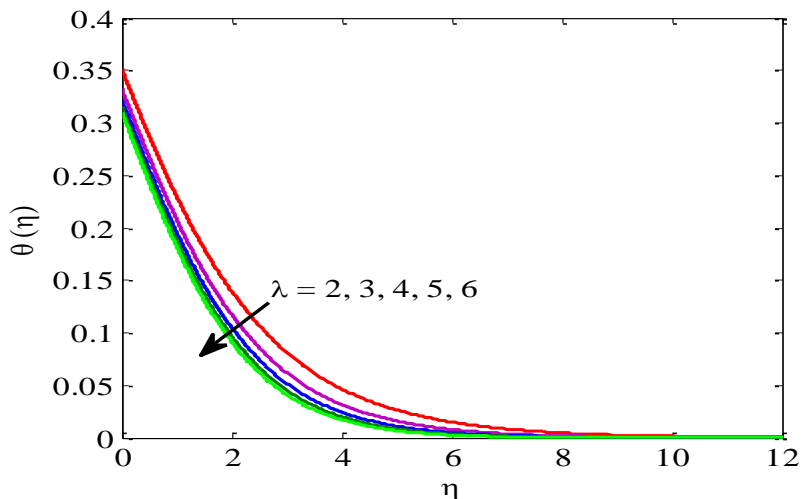


Figure 7: Temperature profiles $\theta(\eta)$ under different values λ .

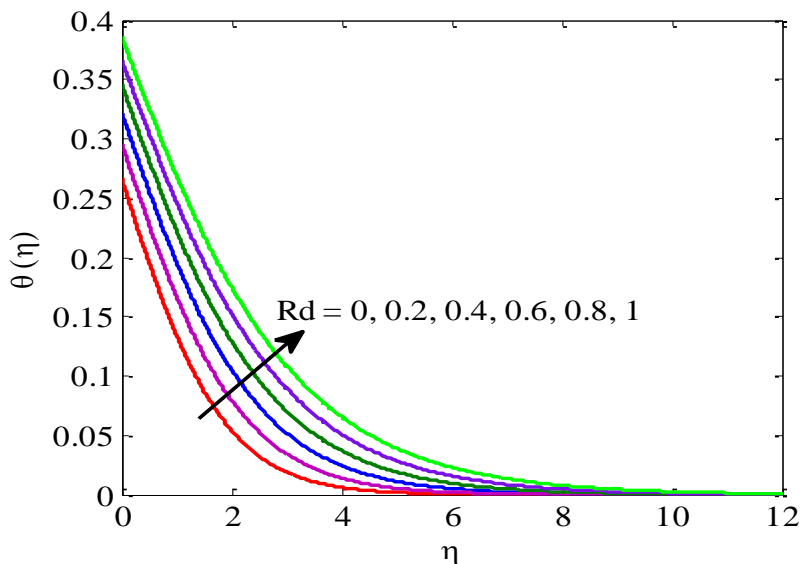


Figure 8: Temperature profiles $\theta(\eta)$ under different values of Rd .

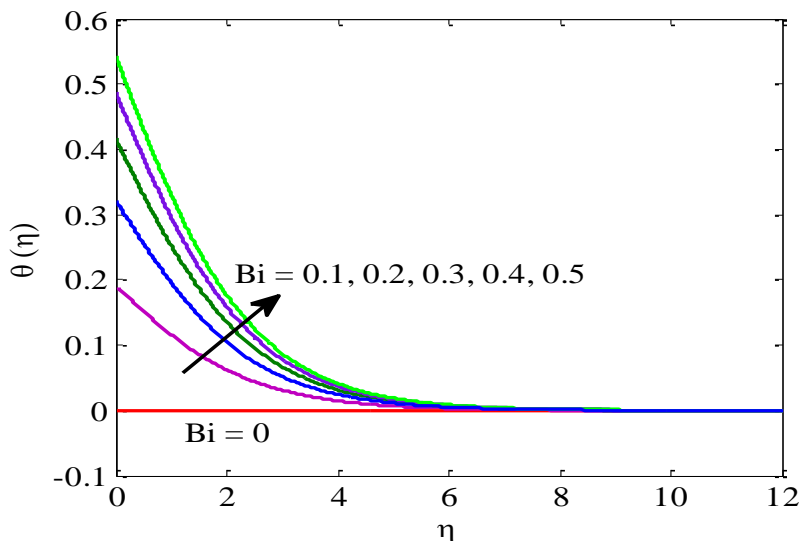


Figure 9: Temperature profiles $\theta(\eta)$ under different values of Bi .

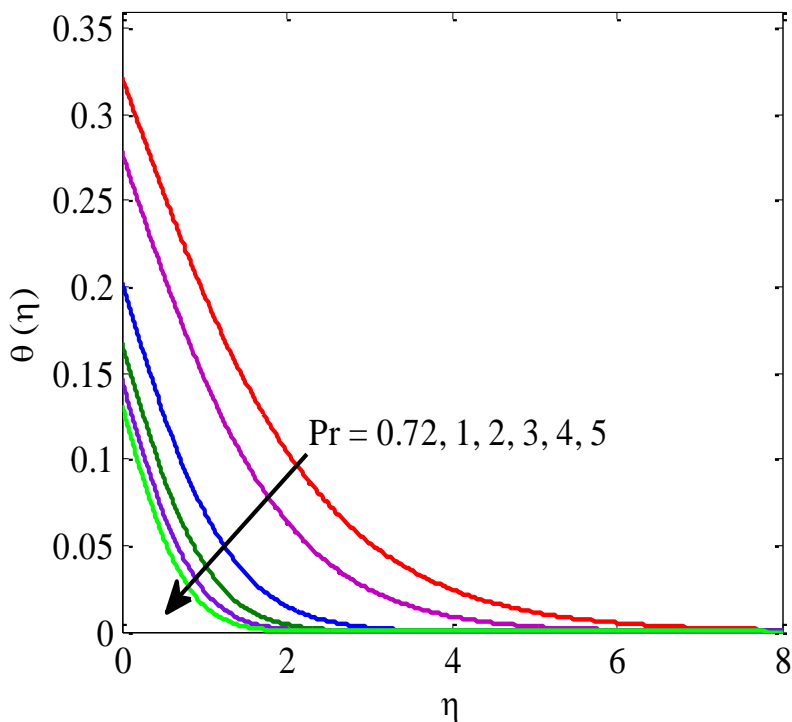


Figure 10: Temperature profiles $\theta(\eta)$ under different values of Pr .

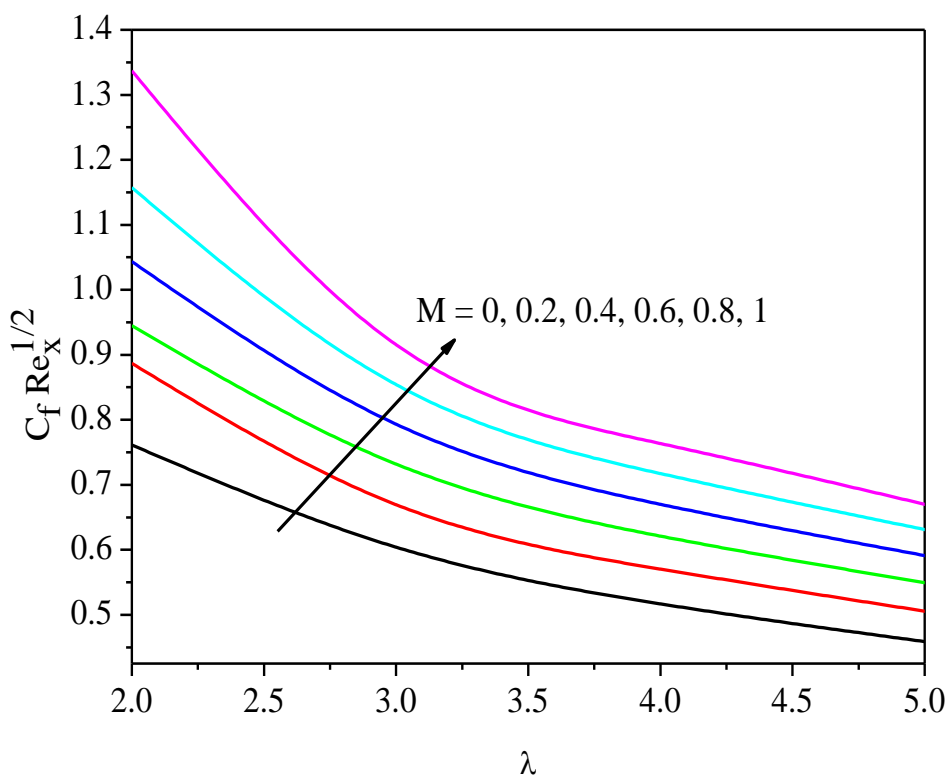


Figure 11: Skin friction coefficient $C_f Re_x^{1/2}$ under different values of M & λ .

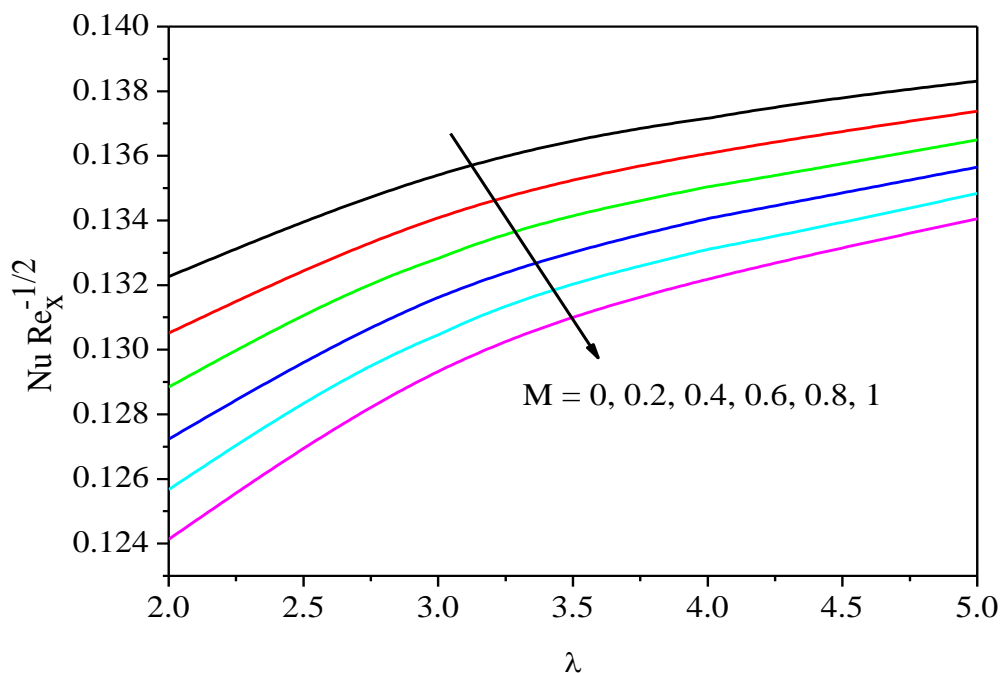


Figure 12: Nusselt number $Nu_x Re_x^{-1/2}$ under different values of M & λ .

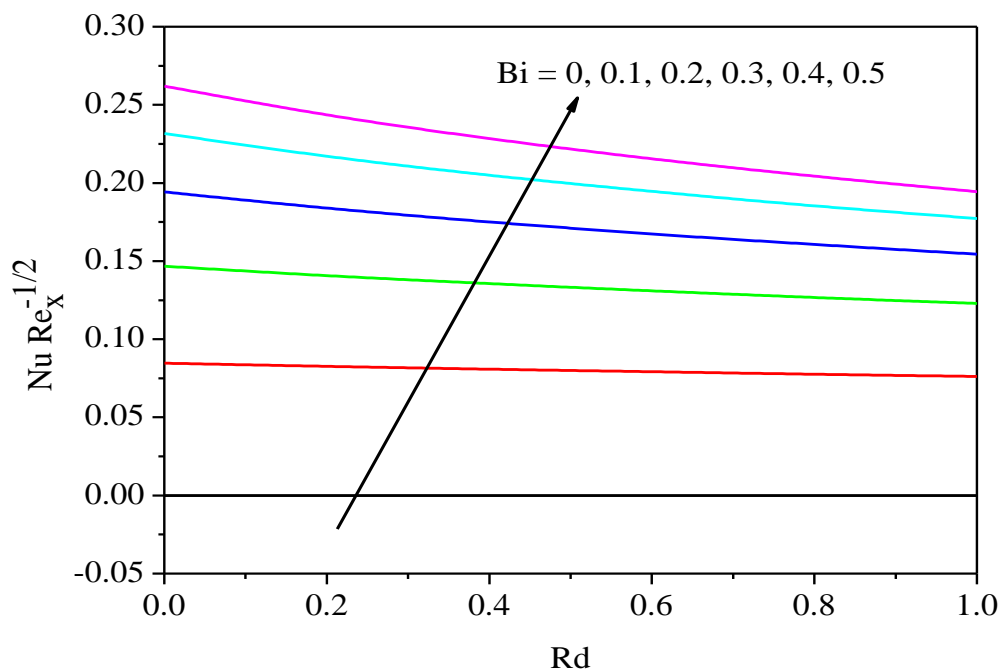


Figure 13: Nusselt number $Nu_x Re_x^{-1/2}$ under different values of Rd & Bi .

Table 1: Comparison of wall shear stress for different M when $\lambda = \xi = 0$.

M	Akbar et al. [3]	Malik et al. [95]	Hussain et al. [65]	Present results
0	-1	-1	-1	-1
1.0	-1.41421	-1.41419	-1.4137	-1.41421356

5.0	-2.44945	-2.44945	-2.4495	-2.44948974
10	-3.31663	-3.31657	-3.3166	-3.31662479
100	-10.04988	-10.04981	-10.0500	-10.04987562
500	-22.38294	-22.38294	-22.3835	-22.38302929
1000	-31.63851	-31.63851	-31.6391	-31.63858404

References:

1. Abd El-Aziz, M., (2009), Radiation Effect on the Flow and Heat Transfer over an Unsteady Stretching Surface, *Int. Commun. Heat Mass Transfer*, Vol. 36, pp.521-524.
2. Akbar, N.S., Ebaid, A. and Khan, Z.H., (2015), Numerical analysis of magnetic field effects on Powell–Eyring fluid flow towards a stretching sheet, *J Magn Magn Mater*, Vol.382, pp.355-358.
3. Ara, A., Khan, N.A., Khan, H. and Sultan, F., (2014), Radiation effect on boundary layer flow of a Powell–Eyring fluid over an exponentially shrinking sheet, *Ain Shams Eng J.*, Vol. 5, pp.1337-1342.
4. Chen, C.K. and Char, M., (1988), Heat Transfer of a Continuous Stretching Surface with Suction or Blowing, *J. Math An. Appl.*, Vol. 135, pp. 568-580.
5. Elbashbeshy, E.M.A., (1997), Heat and Mass Transfer along a Vertical Plate with Variable Surface Tension and Concentration in the Presence of the Magnetic Field, *Int. J. Eng. Sci.*, Vol. 34, pp. 515-522.
6. Erickson, L.E., Fan, L.T., and Fox, V.G., (1996), Heat and Mass Transfer on a Moving Continuous Flat Plate with Suction and Injection, *Ind. Eng. Chem. Fund.*, Vol. 5, pp. 19-25.
7. Ferdows, M., Khalequ, T.S., Tzirtzilakis, E.E. and Sun, Sh., (2017), Effects of Radiation and Thermal Conductivity on MHD Boundary Layer Flow with Heat Transfer along a Vertical Stretching Sheet in a Porous Medium, *Journal of Engineering Thermo physics*, Vol. 26, No. 1, pp. 96-106
8. Ganesh Kumar, K., Giressha, B.J., Manjunatha, S. and Rudraswamy, N.G., (2017), Effect of nonlinear thermal radiation on double-diffusive mixed convection boundary layer flow of visco elastic nanofluid over a stretching sheet, *International Journal of Mechanical and Materials Engineering*, 12:18 DOI 10.1186/s40712-017-0083-5
9. Gangadhar, K., Kannan, T., Sakthivel, G. and Dasaradha Ramaiah, K., (2018), Unsteady free convective boundary layer flow of a nanofluid past a stretching surface using a spectral relaxation method, *International Journal of Ambient Energy*, <https://doi.org/10.1080/01430750.2018.1472648>.
10. Gangadhar, K., Suresh Kumar, Ch. and Ranga Rao, T., (2018), A spectral relaxation approach for diffusion thermo effect on tangent hyperbolic fluid past a stretching surface in the presence of chemical reaction and convective boundary condition, *Computational thermal science*, vol. 10, no.5, pp. 389-403.
11. Ghaly, A.Y., (2002), Radiation Effect on a Certain MHD Free-Convection Flow, *Chaos, Solitons Fractals*, Vol. 13, pp. 1843-1850.
12. Hayat, T., Ali, S., Farooq, M.A. and Alsaedi, A., (2015), On Comparison of series and numerical solutions for flow of Eyring-Powell fluid with Newtonian heating and internal heat generation/absorption, *PLOS One*. doi:10.1371/journal.pone.0129613
13. Hossain, M.A. and Takhar, H.S., (1996), Radiation effects on mixed convection along a vertical plate with uniform surface temperature, *Int. J. Heat Mass Transfer*, Vol.31, pp.243-248.
14. Hussain, A., Malik, M.Y., Bilal, S., Awais, M. and Salahuddin, T., (2017), Computational analysis of magnetohydrodynamic Sisko fluid flow over a stretching cylinder in the presence of viscous dissipation and temperature dependent thermal conductivity, *Results in Physics*, Vol.7, pp.139-146.
15. Ishak, A., Yacob, N. A. and Bachok, N., (2011), Radiation effects on the thermal boundary layer flow over a moving plate with convective boundary condition, *Meccanica*, Vol.46, pp.795-801.

16. Khan, I., Malik, M.Y., Salahuddin, T., Khan, M. and Rehman, K.U., (2017), Homogenous–heterogeneous reactions in MHD flow of Powell-Eyring fluid over a stretching sheet with Newtonian heating, *Neural Computer and Applic.*, Vol.39 (11), pp. 3581-3588.
17. Kim, Y.J., (2004), Heat and Mass Transfer in MHD Micropolar Flow over a Vertical Moving Porous Plate in a Porous Medium, *Transp. Porous Media*, Vol. 56, No. 1, pp. 17-37.
18. Malik, M.Y., Hussain, A. and Nadeem, S., (2013), Boundary layer flow of a Powell–Eyring model fluid due to a stretching cylinder with variable viscosity, *Sci Iran*, Vol. 20, pp.313-321.
19. Malik, M.Y., Salahuddin, T., Hussain, A. and Bilal, S., (2015), MHD flow of tangent hyperbolic fluid over a stretching cylinder: using Keller box method, *J Magn Magn Mater*, Vol.395, pp.271-276
20. Mukhopadhyay, S., (2009), Effect of Thermal Radiation on Unsteady Mixed Convection Flow and Heat Transfer over a Porous Stretching Surface in Porous Medium, *Int. J. Heat Mass Transfer*, Vol. 52, pp. 3261-3265.
21. Nadeem, S. and Saleem, S., (2014), Mixed convection flow of Powell– Eyring fluid along a rotating cone, *Results Phys*, Vol.4, pp.54-62.
22. Nawaz, M., Zeeshan, A., Ellahi, R., Abbasbandy, S. and Rashidi, S., (2015), Joules heating effects on stagnation point flow over a stretching cylinder by means of genetic algorithm and Nelder-Mead method, *Int J Numer Methods Heat Fluid Flow*, Vol.25, pp.665-684.
23. Rajesh Kumar, B., Raghuraman, D.R.S., and Muthucumaraswamy, R., (2002), Hydromagnetic Flow and Heat Transfer on a Continuously Moving Vertical Surface, *Acta Mech.*, Vol. 153, pp. 249-253.
24. Raptis, A. and Kafoussias, N.G., (1982), Magnetohydrodynamic Free Convection Flow and Mass Transfer through Porous Medium Bounded by an Infinite Vertical Porous Plate with Constant Heat Flux, *Can. J. Phys.*, Vol. 60, no. 12, pp.1725-1729.
25. Raptis, A. and Massalas, C.V., (1998), Magnetohydrodynamic Flow past a Plate by the Presence of Radiation, *Heat Mass Transfer*, Vol. 34, pp. 107-109.
26. Raptis, A., (2017), Effects of Thermal Radiation on the MHD Flow Past a Vertical Plate, *Journal of Engineering Thermophysics*, Vol. 26, No. 1, pp. 53-59
27. Rosca, A.V. and Pop, I., (2014), Flow and heat transfer of Powell–Eyring fluid over a shrinking surface in a parallel free stream, *Int J Heat Mass Transf.*, Vol. 71, pp.321-327.
28. Sakiadis, B.C., (1961), Boundary Layer Behavior on Continuous Solid Surface: I. The Boundary Layer Equation for Two-Dimensional and Axi-Symmetric Flow, *AIChE J.*, Vol. 7, No. 1, pp. 26-28.
29. Sattar, M.A., Rahman, M.M. and Alam, M.M., (2000), Free Convection Flow and Heat Transfer through a Porous Vertical Flat Plate Immersed in a Porous Medium, *J. Energy Res.*, Vol. 22, No. 1, pp. 17-21.
30. Shateyi, S., Sibanda, P., and Motsa, S.S., (2017), Magnetohydrodynamic Flow past a Vertical Plate with Radiative Heat Transfer, *J. Heat Transfer*, Vol. 129, No. 12, pp. 1708-1713.
31. Takhar, H.S., Gorla, R.S.R., and Soundelgekar, V.M., (1996), Non-linear One-Step Method for Initial Value Problems, *Int. Num. Meth. Heat Fluid Flow*, Vol. 6, pp. 22-83.
32. Whitaker, S., (1980), Radiant Energy Transport in Porous Media, *Int. Eng. Chem. Fund.*, Vol. 19, pp. 210–218.